Received: 5 August 2022 | Revised: 18 September 2022 | Accepted: 25 September 2022

DOI: 10.1002/app.53260

RESEARCH ARTICLE

Applied Polymer SCIENCE WILEY

Novel multifunctional microcapsule and its cyanate ester resin composites with self-healing ability and gamma radiation shielding ability

Yuehao Rui[1] | Feida Chen[1,2] | Minghao Zhao[1] | Jing Zhong[1] | Yong Li[3] | Xiaobin Tang[1,2]

[1]Department of Nuclear Science and Technology, Nanjing University of Aeronautics and Astronautics, Nanjing, China

[2]Key Laboratory of Nuclear Technology Application and Radiation Protection in Astronautics, Ministry of Industry and Information Technology, Nanjing, China

[3]College of Materials Science and Technology, Nanjing University of Aeronautics and Astronautics, Nanjing, China

Correspondence
Feida Chen and Xiaobin Tang, Department of Nuclear Science and Technology, Nanjing University of Aeronautics and Astronautics, Nanjing 211106, China.
Email: fdchen@nuaa.edu.cn and tangxiaobin@nuaa.edu.cn

Funding information
Fundamental Research Funds for the Central Universities, Grant/Award Number: NS2021036; Postdoctoral Research Foundation of China, Grant/Award Number: 2020M671488; Postgraduate Research & Practice Innovation Program of NUAA, Grant/Award Number: xcxjh20210622

Abstract

Resin-based composites used in spacecraft face risks from space debris and high-energy charged particles during their long-term service in the space environment. This work proposes a novel microcapsule (MC) and its cyanate ester (CE) resin-based composites (CE/MCs) with self-healing ability and gamma radiation shielding ability. The multifunctional epoxy/lead tungstate (EP@PWO) microcapsules are developed through self-assembly method and in-situ precipitation method. These microcapsules and curing agent 4,4′-diaminodiphenylsulfone (DDS) are incorporated into the CE resin to form resin-based composites with low curing temperature, self-healing ability, and gamma radiation shielding ability. Various approaches including chemical characterizations (X-ray diffractometer, fourier-transform infrared, energy dispersive spectrometer), microscopy (optical microscope, scanning electronic microscope), and thermal analysis (differential scanning calorimeter, thermogravimetric analysis) are utilized to demonstrate the successful encapsulation of the EP resin by PWO shell and good thermal stability of this material. The mechanical property, self-healing ability, and gamma radiation shielding property are investigated via fracture toughness test and using a NaI (Tl) spectrometer. In comparison with pure CE resin, the fracture toughness of the CE/MCs composites can increase by 66.5%, and the self-healing efficiency can reach up to 56%, indicating that the microcapsules have good toughening and self-healing abilities. The microcapsules and their composites also exhibit good gamma radiation shielding properties.

KEYWORDS

applications, composites, mechanical properties, thermosets

1 | INTRODUCTION

With the advancement of the aerospace industry, the issue of space radiation shielding has received widespread attention. In comparison with traditional aluminum alloys,[1,2] resin-based composites have lower atomic number, which can significantly reduce the secondary gamma rays after shielding against high-energy proton and electron radiation. These composites also have light-weight and high-strength characteristics,[3]

which are ideal structural and functional integrated materials for space radiation shielding. Cyanate ester (CE) resins are often used as the matrix material of resin-based composites because of their good mechanical strength, dielectric properties and excellent processing and forming properties.[4] These composites also have a wide range of applications in spacecraft structural materials,[5] solar wing substrates,[6] and space optical systems.[7] However, CE composites have some problems as shielding materials in space environments. On the one hand, CE resins contain plenty of low atomic number elements, such as H and O, which have good shielding effects on high-energy protons and electrons. But CE resins are not as good at shielding secondary gamma rays generated by the interaction of protons and electrons with other materials as aluminum alloys, which may result in an increase in the total ionizing dose on the internal components of the spacecraft.[8] On the other hand, CE resins have poor fracture toughness and are prone to microcracks under service loads, thus destroying the structural integrity of the materials.[9,10] Meanwhile, spacecraft serve in a complex space environment, especially in low Earth orbit, which mainly includes high-vacuum and high-energy charged particle irradiation.[11,12] High-energy electrons and protons irradiation further exacerbate the embrittlement of CE resins, which poses a great threat to the normal operation, in-orbit reliability, as well as the lifetime of spacecraft and is one of the main causes of spacecraft material degradation and damage.[13,14]

Given that CE resins are inherently brittle,[15] and the space environment exacerbates the embrittlement, microcracks can easily appear within the resin during spacecraft service, which could seriously damage the structural integrity of the materials. These microcracks must be suppressed or repaired. Various methods can be used to improve the fracture toughness of CE resins, thereby suppressing the expansion of microcracks. The approaches include the formation of an interpenetrating network with thermoplastic resin by blending,[16,17] addition of rubber inclusions,[18,19] and copolymerization with thermosetting resins.[20–22] However, when cracks started to propagate inside the material, localized filling repair methods have to be used to solve this issue. These methods include the plug/patch repairs, bolted plates, and injecting resins.[23] Nevertheless, these methods are difficult to operate and cannot in-situ repair micro damage within the material, thus adding extra weight to the structure. Another approach is to incorporate microcapsules containing healing agents.[24,25] This extrinsic self-healing concept was first proposed by White et al.[26] When microcracking occurs in the material, the expansion of the cracks causes the microcapsules to rupture and release a healing agent to self-repair the microcrack. Yuan et al.[27] first reported the use of epoxy/poly(urea–formaldehyde) (EP@PUF) microcapsules for the self-healing of CE resin, and they found that the addition of appropriate microcapsules not only imparts self-healing capability to the materials but also increases the fracture toughness. Gu et al.[28] fabricated cyanate ester/polyglycidyl methyacrylate (CE@PGMA) microcapsules for the self-healing of EP resin, which also exhibited excellent self-healing property. Although it has been demonstrated that CE resins and EP resins can repair each other, such composites with only self-healing function cannot meet the requirements of spacecraft. The harsh physical environment and complex radiation environment in space require structural materials to have not only excellent mechanical property but also shielding ability against mixed radiation fields. The traditional method for enhancing the gamma radiation shielding ability of resin-based composites is to add fillers with high atomic number elements, such as lead, tungsten, and tin.[29] Lou et al.[30] encapsulated paraffin (Pn) with lead tungstate (PWO) shell to prepare phase change materials with gamma radiation shielding function. The advantage of PWO shell over common microcapsule shell materials is that it not only enhances the thermal stability of the microcapsules, but also imparts excellent gamma radiation shielding capability to them. However, at present, there is no relevant report on microcapsules with both self-healing function and gamma radiation shielding function. Multifunctional composites with self-healing function and excellent radiation shielding function can be obtained by adding self-healing microcapsules and radiation shielding fillers to the resin matrix. However, adding different kinds of fillers to the resin matrix may result in un-even distribution of the fillers and greatly increase the weight of the material, which is incompatible with the requirement for a light-weight spacecraft.[31] Hence, a light-weight, high-strength material with self-healing capability and effective gamma radiation shielding capability must be developed.

In this work, we prepare a microcapsule with self-healing ability and gamma radiation shielding ability. We can obtain multifunctional composites by incorporating such microcapsules as fillers into the resin matrix. This new microcapsule with PWO shell and EP core material is prepared via self-assembly method and in-situ precipitation method, and mixed with DDS in CE resins to prepare a new multifunctional resin-based composite material with self-healing ability and radiation shielding ability. When microcracks occur in the matrix, they will destroy the microcapsules containing the healing agent. The healing agent will react with the curing agent DDS buried in the resin matrix to repair the broken area. The PWO shell of the microcapsules enhances the gamma

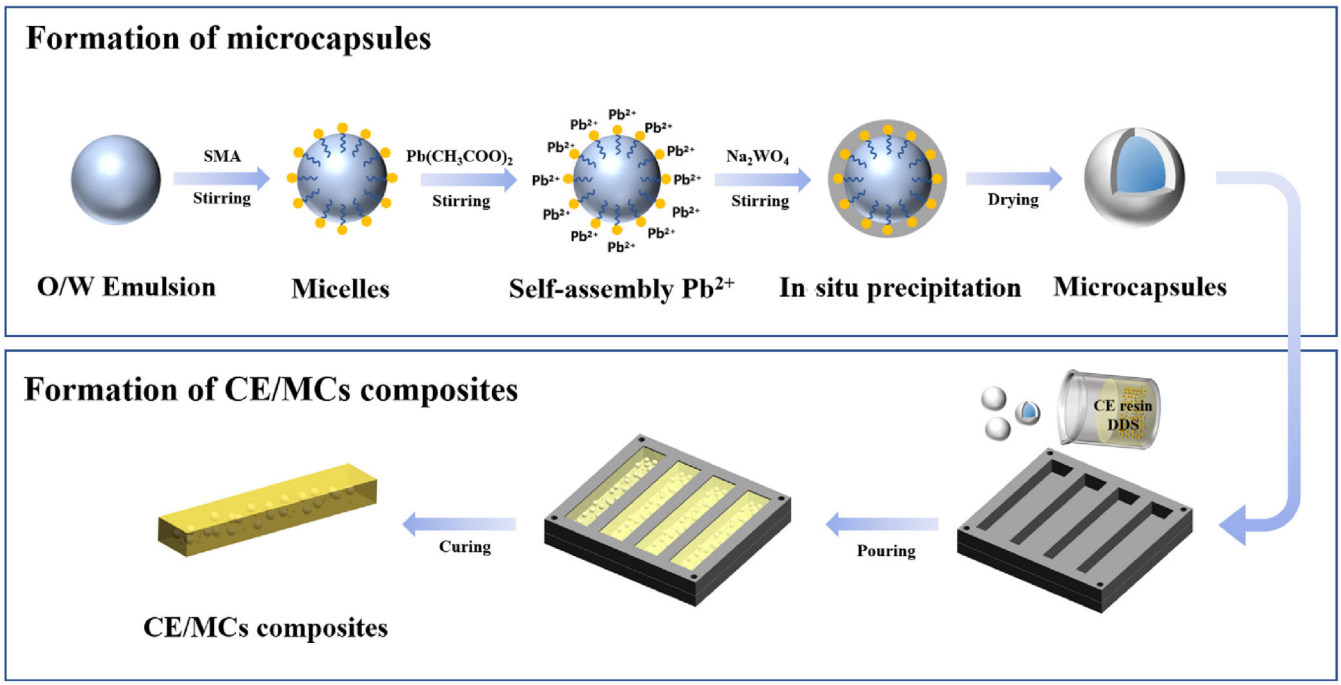

FIGURE 1 Formations of microcapsules and CE/MCs composites. CE/MCs, cyanate ester resin-based composites containing microcapsules [Color figure can be viewed at wileyonlinelibrary.com]

radiation shielding capability of the composites. This multifunctional microcapsule and its CE resin-based composites have the potential to be the next generation structural materials for spacecraft.

2 | EXPERIMENTAL SECTION

2.1 | Materials

Bisphenol A epoxy resin (EP) was purchased from Kunshan Jiulimei Electronic Materials Co., Ltd (Suzhou, China). Bisphenol A dicyanate (CE) was purchased from Norna Chemical Co., Ltd (Wuhan, China). Triethanolamine (TEA), Lead (II) acetate trihydrate (Pb $[CH_3COO]_2{\cdot}3H_2O$), sodium tungstate dihydrate ($Na_2WO_4{\cdot}2H_2O$), styrene–maleic anhydride copolymer (SMA, Mn ~ 28,000), and 4,4′-diaminodiphenylsulfone (DDS) were purchased from Macklin Biochemical Co., Ltd. (Shanghai, China).

2.2 | Preparation of microcapsules

As shown in Figure 1, the microencapsulated EP with PWO shell was synthesized in an oil-in-water (O/W) emulsion templating system. The synthetic procedure is described as follows: in a 100 ml beaker, SMA (1.45 g), E51 epoxy (10 g), and appropriate amount of TEA were added into deionized water (75 ml), pH was controlled at 8–9, and magnetically stirred at 80 °C for 10–20 min. Then, the emulsion was placed on a homogenizer and stirred at 16,000 rpm for 3 min. The emulsified EP resin emulsion was then transferred to a 500 ml flask and magnetically stirred at 65°C. Subsequently, lead acetate (Pb $[CH_3COO]_2$) solution (9.63 g, 140 ml) was added and stirred at 500 rpm for 3 h. Thereafter, sodium tungstate (Na_2WO_4) solution (8.35 g, 140 ml) was added and stirred at 500 rpm for 8 h. Finally, the microcapsules were washed three times with deionized water and anhydrous ethanol, and then dried in a blast oven at 60 °C for 48 h.

2.3 | Preparation of CE/MCs composites

As shown in Figure 1, The CE resin-based composites are prepared using the mold casting method. The formation procedure is described as follows: in a 200 ml beaker, CE resins were added and heated to 100°C. Until the CE resin powder melts to a clear liquid, 1 wt% DDS was added and magnetically stirred at 120°C for 30–40 min. Then, EP@PWO microcapsules (2.5, 5.0, 7.5, 10.0, and 12.5 wt%) were added, and the mixture was stirred for 10–20 min. After that, the resin mixture was poured into a pre-heated mold, and the mold was placed in a vacuum drying oven for degassing, and curing according to the following schedule: 130°C/2 h + 150°C/2 h + 180°C/2 h.[27] The samples were slowly cooled to room temperature in the oven after curing.

2.4 | Characterization

The chemical structures of the EP resin, PWO, and EP@PWO microcapsules were characterized using Fourier-transform infrared (FTIR/Nicolet iS5) spectra. The spectra were taken on a transition mode in the 4000–400 cm^{-1} range. The crystalline structures of the shell materials and EP@PWO microcapsules were determined with an X-ray diffractometer (XRD/Bruker D8 Advance diffractometer) with a 2θ scan range of 5°–90° and scan speed of 5°/min. The surface features of the EP@PWO microcapsules and CE/MCs composites were investigated by an optical microscope (OM/MR5000) and a scanning electronic microscope (SEM/Hitachi S-4800). The particle size of the microcapsules was measured with a laser particle size scanner (Malvern Mastersizer 2000). The thermal behavior of the EP resin and the as-prepared microcapsules were measured with a differential scanning calorimeter (DSC/NETZSCH DSC 200 F3). The samples were heated from 30°C to 500°C at 10°C/min under a pure nitrogen atmosphere. The flow rate of nitrogen gas was 20 ml/min. The thermal stability of the EP resin and the as-prepared microcapsules was characterized by thermogravimetric analysis (TGA/NETZSCH STA 449 F5). The samples were heated from 30°C to 700°C at 10°C/min under a pure nitrogen atmosphere. The flow rate of nitrogen gas was 50 ml/min.

2.5 | Fracture toughness testing and evaluation of self-healing efficiency

The fracture toughness (K_{IC}) was measured by using standard single-edge notched beam (SENB) specimens under mode I fracture conditions. First, use a grinder to cut a notch in the middle part of the specimen, then use a razor to lightly tap the bottom of the notch to create a pre-crack. The size of the original crack was $0.45\ W < a < 0.70\ W$. After the specimens were tested at a constant 0.5 mm/min displacement rate until fracture and healed at 200°C for 1 h, the healed specimens were examined by using the same experimental parameters. Eight samples were tested for each component. K_{IC} was calculated using[27]:

$$K_{IC} = Y\frac{3PS\sqrt{a}}{2BW^2}, \tag{1}$$

where P is the critical load, B is the thickness, W is the width, S is the span, and Y is defined as follows:

$$Y = 1.93 - 3.07\left(\frac{a}{W}\right) + 14.53\left(\frac{a}{W}\right)^2 - 25.11\left(\frac{a}{W}\right)^3 + 25.80\left(\frac{a}{W}\right)^4, \tag{2}$$

The healing efficiency (η) of the specimens was calculated using[26]:

$$\eta = \frac{K_{IC\ healed}}{K_{IC\ origin}} = \frac{\text{Healed specimen's fracture toughness}}{\text{Original specimen's fracture toughness}}, \tag{3}$$

2.6 | Gamma radiation shielding performance testing

The experimental device for the gamma radiation shielding performance test is shown in Figure 2. ^{133}Ba (80 and 356 keV) and ^{137}Cs (662 keV) sources with collimators were used as gamma sources. A gamma spectrometer, which consists of 3″ × 3” NaI (Tl) crystal, Al shell, and DigiBASE, was used for testing the gamma radiation shielding performance of the microcapsules and CE/MCs composites. Certain amounts of microcapsule powder were pressed into a 1 cm-diameter mold to obtain samples with a thickness of 5 mm. Direct resin-based composites were used for the composite samples. The gamma ray transmission factor (I_0/I) was measured by varying the thickness for all the samples. The attenuation of photons is governed by the following relationship:

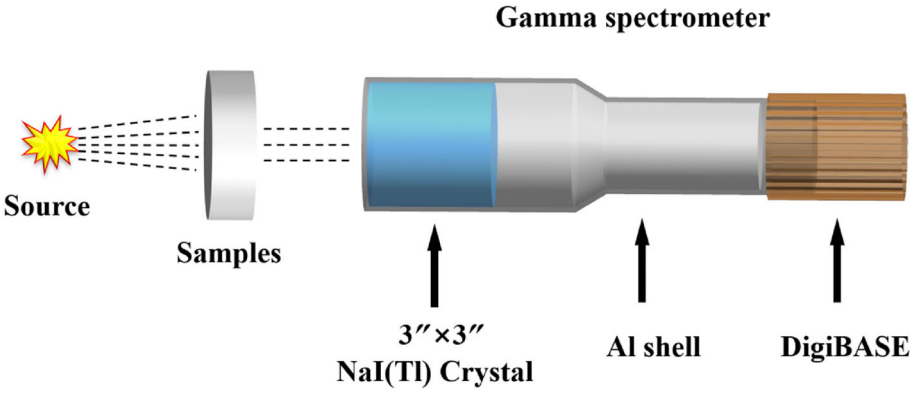

FIGURE 2 Experimental device for gamma radiation shielding performance test [Color figure can be viewed at wileyonlinelibrary.com]

$$I = I_0 e^{-\mu\delta}, \quad (4)$$

where I denotes the transmitted photon radiation intensities, and I_0 is the incident one; μ is the linear attenuation coefficient; and δ is the thickness (cm) of the samples.

Considering the density of the different samples, the mass attenuation coefficient was calculated using:

$$\mu_m = \frac{\mu}{\rho}, \quad (5)$$

where μ_m is the mass attenuation coefficient, and ρ is the density (g/cm^3) of the samples.

3 | RESULTS AND DISCUSSION

3.1 | Characterization of microcapsules

The chemical contents of the microcapsules were measured by XRD and FTIR. The XRD patterns of the microcapsules and PWO are shown in Figure 3a. The diffraction peaks of the microcapsules at 2θ = 27.55°, 29.78°, 32.90°, 44.92°, and 55.45° are attributed to the diffraction of the planes (112), (004), (200), (204), and (312) of PWO, respectively. This result indicated that microcapsules have the PWO component.

The FTIR spectra of the microcapsules, PWO, and EP resin are shown in Figure 3b. The PWO shell materials were obtained by grinding the microcapsules in a mortar and washing with acetone, which can remove the EP resin core. The peaks at 1476, 2856, 2920, and 2975 cm^{-1} belong to characteristic peaks of stretching vibrations of alkyl C—H belonging to —CH_3 and —CH_2, confirming the existence of EP resin as a hydrocarbon substance, and the peak at 779 cm^{-1} reflects the stretching vibration of W—O in PWO.[32] The characteristic peaks of EP resin and PWO are also reflected in the FTIR spectrum of the microcapsules. The FTIR results indicated that the microcapsules are composed of EP resin and PWO.

3.2 | Morphology and microstructure of microcapsules

Figure 4a,b shows the optical image and SEM image of the microcapsules, respectively. The figures demonstrate that the microcapsule samples show an irregular spherical shape with a dense shell. The surface roughness is due to the high content of Pb^{2+} and WO_4^{2-} ions in the EP resin emulsion, resulting in the rapid precipitation of PWO and the formation of a dense PWO shell layer on the EP resin surface. The surface morphology of the broken microcapsules is shown in Figure 4c, and the partial magnification of the broken region is illustrated in the small picture. The PWO shell of the microcapsules has a dense layer, while the EP resin core has a fluid shape. Figure 4d shows the SEM image and EDS mappings of the microcapsules in the CE resins. The microcapsule shows a distinct core–shell structure. According to the EDS mapping spectra, Pb, W, and O atoms existed in the shell of capsules, demonstrating that the shell was largely composed of PWO. The particle size statistics of the microcapsules are shown in Figure 4e, and the average size is around 43.6 μm.

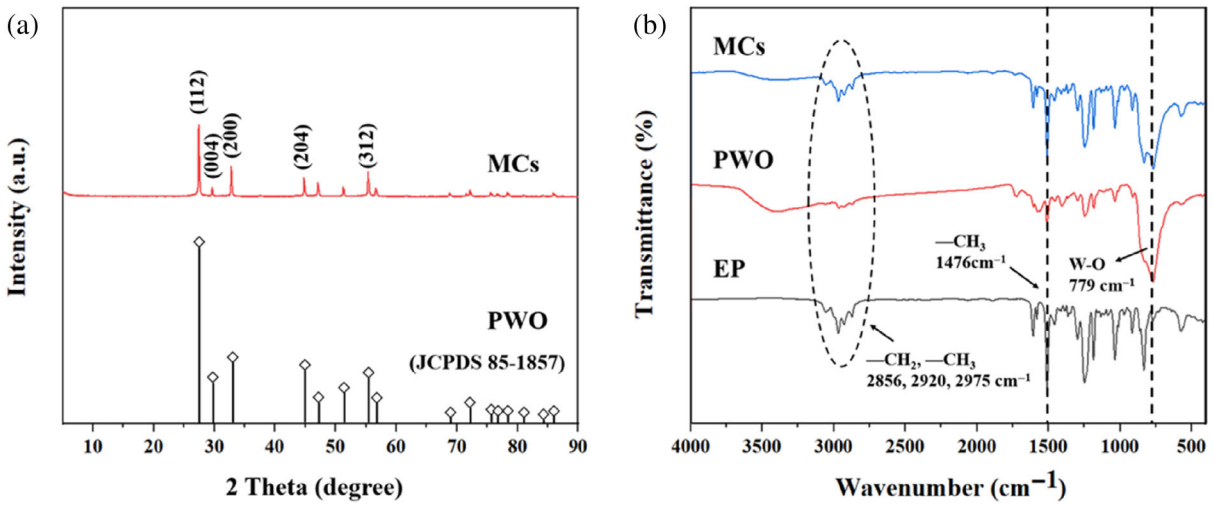

FIGURE 3 (a) XRD pattern of microcapsules, (b) FTIR spectra of EP resin, PWO, and microcapsules. EP, epoxy; FTIR, Fourier-transform infrared; PWO, lead tungstate; XRD, X-ray diffractometer [Color figure can be viewed at wileyonlinelibrary.com]

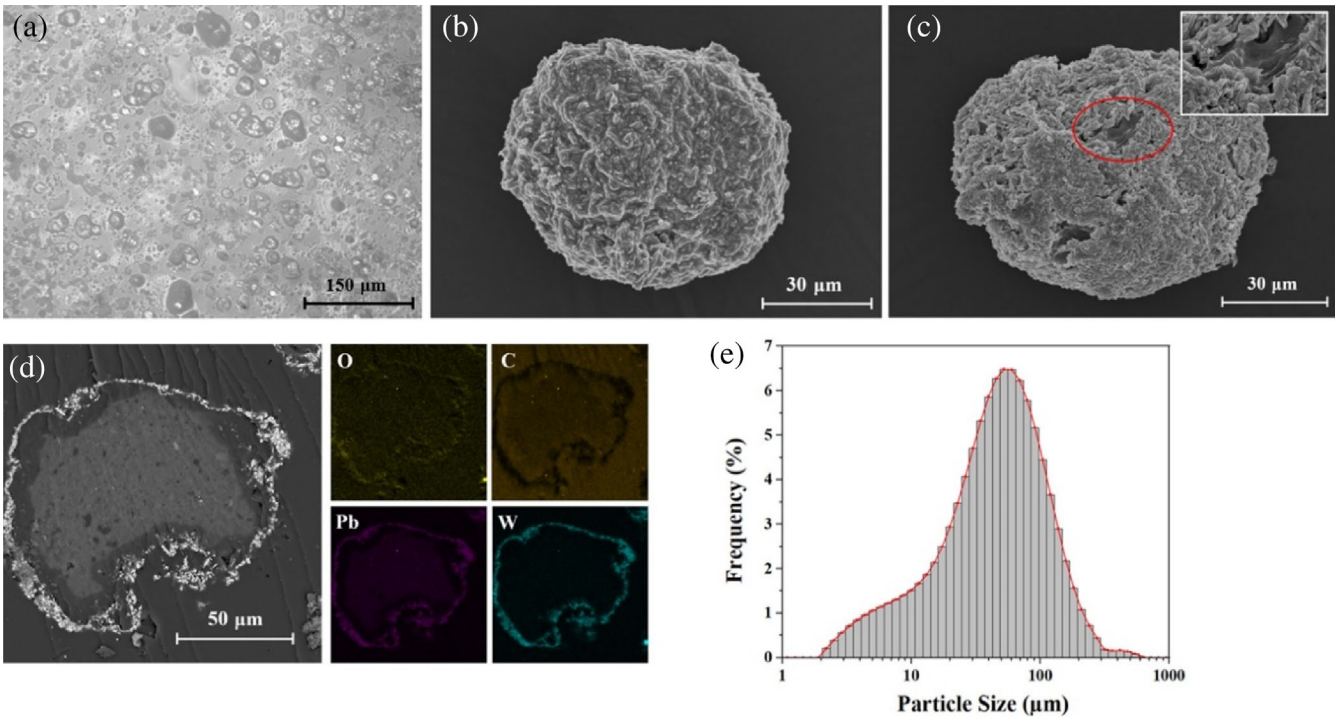

FIGURE 4 (a) Optical image of microcapsules, (b) SEM image of complete microcapsule, (c) SEM image of broken microcapsule, (d) SEM image and EDS mappings of microcapsules in CE resin, and (e) particle size distribution of microcapsules. CE, cyanate ester; EDS, energy dispersive spectrometer; SEM, scanning electronic microscope [Color figure can be viewed at wileyonlinelibrary.com]

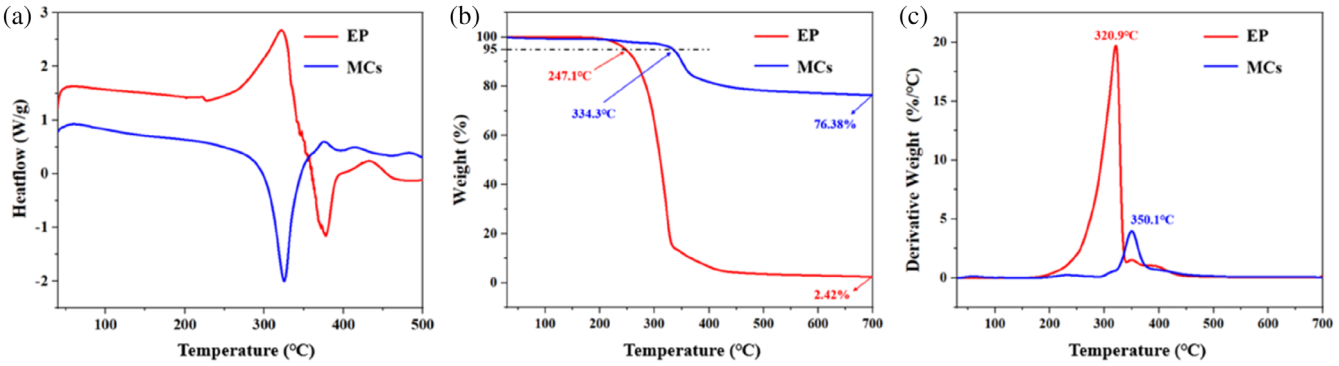

FIGURE 5 (a) DSC curves, (b) TGA curves, and (c) DTG curves of EP resin and microcapsules. DSC, differential scanning calorimeter; DTG, differential thermogravimetric; EP, epoxy; TGA, thermogravimetric analysis [Color figure can be viewed at wileyonlinelibrary.com]

3.3 | Thermal properties of microcapsules

Figure 5a shows the DSC curves of the EP resin and microcapsules. An obvious exothermic peak and heat absorption peak can be found in the DSC curves of microcapsules from 50°C to 450°C. The exothermic peak around 326°C consists of two parts of reaction, one is the curing reaction between the EP resin and the residual anhydride SMA from the previous preparation process, and the other is the self-etherification reaction of the EP resin at high temperature. The tiny heat absorption peak around 360°C is caused by the further decomposition of the residual substances in the microcapsules.

Figure 5b,c shows the TGA and DTG (differential thermogravimetric) curves of the EP resin and microcapsules. The decomposition temperature (T_d) at 5% weight loss and the temperature of the maximum rate of weight loss (T_{max}) for the EP resin are 247.1°C and 320.9°C, respectively. The T_d and T_{max} of the microcapsules are 334.3°C and 350.1°C, respectively. The results indicate the enhanced thermal stability of the microcapsules. The existence of inorganic PWO shell suppresses the decomposition of EP resin and enhances the heat-resistant

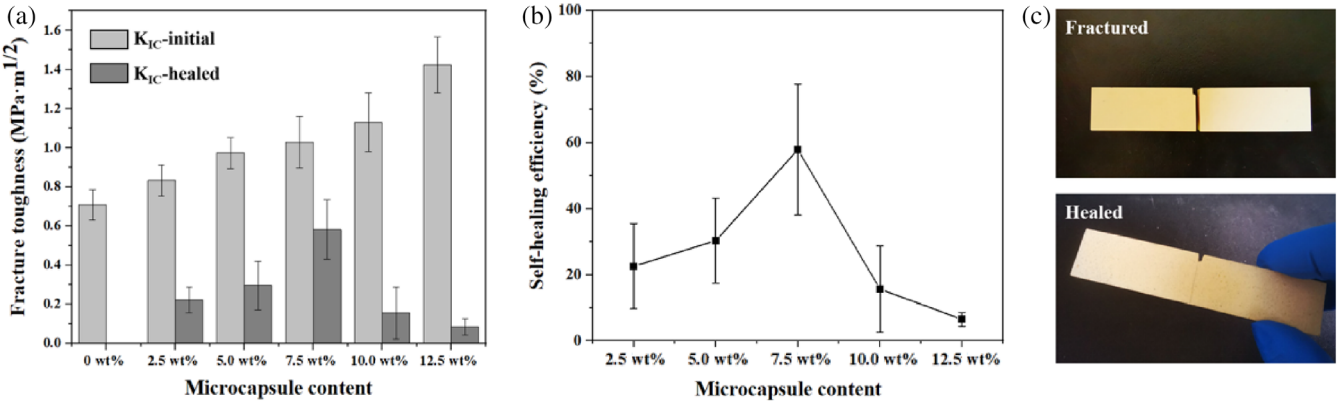

FIGURE 6 (a) Fracture toughness and (b) self-healing efficiency of CE/MCs composites with different contents of microcapsules, and (c) photos of fractured composite and healed composite. CE/MCs, cyanate ester resin-based composites containing microcapsules [Color figure can be viewed at wileyonlinelibrary.com]

ability of microcapsules. The as-prepared microcapsule was washed with acetone to determine the encapsulation efficiency of the microcapsules, and it showed a statistical encapsulation efficiency of 24% calculated by mass. When converted to volume calculation, the encapsulation efficiency of the microcapsule is 69% due to the high density of the shell layer. This high encapsulation loading is just one requirement underlying the high self-healing efficiency of microcapsules.

3.4 | Self-healing ability of CE/MCs composites

The fracture toughness of the CE/MCs composite is shown in Figure 6a. The CE/MCs composites show increased fracture toughness compared with the pure CE resins (0 wt%). The original fracture toughness ($K_{IC\ origin}$) increases by 17.5%, 37.3%, 45.1%, 27.6%, and 66.5% with 2.5, 5.0, 7.5, 10.0 wt%, and 12.5 wt% microcapsules, respectively. The toughening ability of the CE/MCs composites comes from two aspects. On the one hand, the EP resin reacts with the triazine rings in the CE resin matrix to form oxazolidinone rings, and the new cross-linked network increases the molecular chain stiffness, which is macroscopically expressed as an increase in material fracture toughness.[27] On the other hand, the microcapsules are added as fillers diffusely distributed in the resin matrix. When the resin produces microcracks, the microcapsules will suppress their expansion. After the healing schedule (200°C/1h), the healed fracture toughness ($K_{IC\ healed}$) recovers by 22.6%, 30.4%, 56.0%, 6.5%, and 5.0% with the composites containing 2.5, 5.0, 7.5, 10.0, and 12.5 wt% microcapsules, respectively. The self-healing capability of the CE/MCs composites arises from the release of uncured EP resin from the ruptured microcapsules, which subsequently reacts with the residual amine curing agent in the matrix to polymerize resin and re-bonds the cracked surface. The self-healing efficiency (η) of the composites first increases and then decreases with the increase in the microcapsule content (Figure 6b). The increase in η is due to the increased amount of EP resins, resulting in more extensive coverage and bonding of cracked surfaces. It is speculated that the reason for the decrease of η is that the high microcapsule content affects the flow of the healing agent and prevents the healing agent from smoothly reaching the microcrack area.

The integrity and dispersibility of the microcapsules in the resin matrix are crucial for the healing properties of the microcapsule-based self-healing materials. The dispersion of the microcapsules in the resin matrix was investigated from the cross-sectional SEM images of the pure CE resin and CE/MCs composites. In Figure 7a, the cross-section of the pure resin is smooth with obvious faults. By contrast, the microcapsules in Figure 7b are diffusely distributed in the resin. The intact microcapsules (broken and irregular microcapsules) and dislodged PWO shell fragments can be observed. The small picture in Figure 7b shows a broken microcapsule in one portion of the shell, and the rough PWO shell and EP resin can be clearly observed. The fracture pattern of the resin matrix is obscured due to the distribution of the microcapsules, which can also indicate that the microcapsules can effectively suppress the crack expansion. The self-healing performance can be judged more intuitively by observing the changes in the fractured section after being repaired. In Figure 7c,d, the cured EP resin filled some of the cracks, although some gaps can still be observed around the cracks, indicating that the microcapsules' self-healing system cannot achieve the complete filling of the cracks, which is possibly attributed to the large particle size of the microcapsules and the long spacing between different microcapsules.

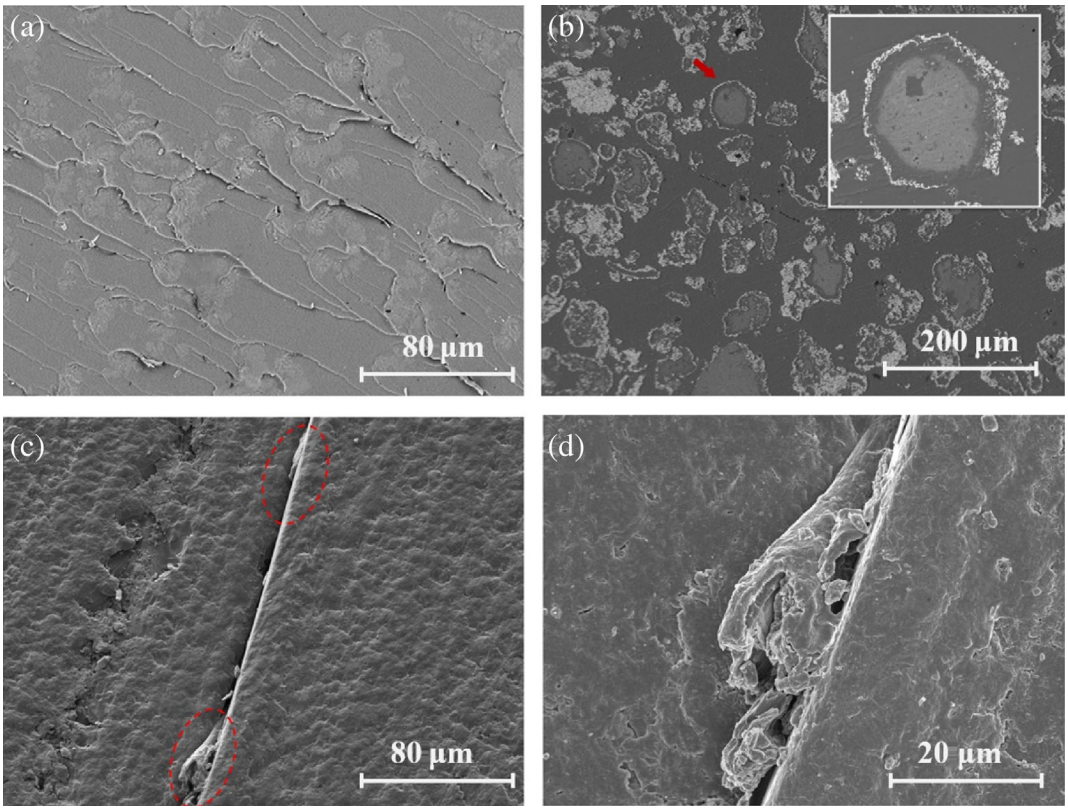

FIGURE 7 SEM images of the (a) pure CE resin section and (b) CE/MCs composite section after the fracture toughness test, (c) fractured surfaces after being repaired, and (d) healing area. CE/MCs, cyanate ester resin-based composites containing microcapsules; SEM, scanning electronic microscope [Color figure can be viewed at wileyonlinelibrary.com]

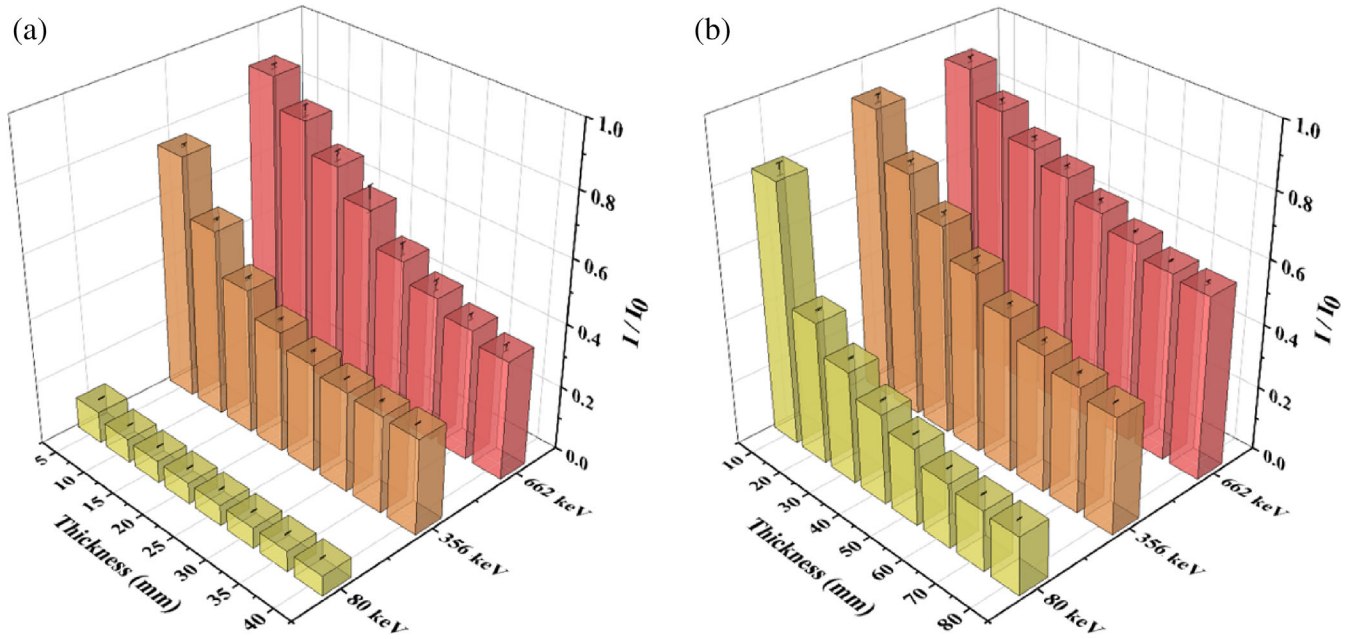

FIGURE 8 Gamma radiation transmittance of the (a) microcapsules and (b) 2.5 wt% microcapsule content of the CE/MCs composites with different thicknesses for the different gamma radiation energies. CE/MCs, cyanate ester resin-based composites containing microcapsules [Color figure can be viewed at wileyonlinelibrary.com]

3.5 | Gamma shielding performance of microcapsules and CE/MCs composites

The gamma radiation transmittance of the microcapsules and CE/MCs composites is displayed in Figure 8. Under the same gamma radiation energy, the gamma radiation transmittance calculated by I/I_0 decreases with the thickness of the samples. The incident photons need to pass through a longer shield material as the thickness increases, and the attenuation rate will be greater. The shielding ability of the microcapsules is better than that of the CE/MCs composites, especially at low energy (80 keV). This case is because the PWO shell of the microcapsules is the effective ingredient shielding gamma radiation, and the more shielding components per unit volume, the more effective the absorption of photons. Under the same thickness of the sample, the shielding ability weakens with the increasing energy of gamma radiation.

Figure 9 shows the gamma shielding properties of the CE/MCs composites reflected by the linear and mass attenuation coefficients at the different gamma radiation energies. The linear attenuation coefficient values in Figure 9a increase with increasing microcapsule content. The minimum values are 0.11546, 0.11319, and 0.10293 cm^{-1} at 80, 356, and 662 keV energy. Meanwhile, the maximum values are 0.53185, 0.27796, and 0.12619 cm^{-1} at 80, 356, and 662 keV energy. The gamma radiation shielding capacity of the CE/MCs composite material was improved by up to 364.25%, 145.57%, and 22.27% at 80, 356, and 662 keV energy compared with the pure CE resin. This result can be attributed to the microencapsulated filler with PWO shell being uniformly dispersed in the matrix, which enhances the chance of interaction with photons and increases the attenuation coefficient of the composites. The increasing trend of the mass attenuation coefficient values in Figure 9b is consistent with the increasing trend of the linear attenuation coefficient at low energies (80 and 356 keV). However, the values show a fluctuating trend at high energy (662 keV). The minimum values are 0.09145 and 0.09139 cm^2/g at 80 and 356 keV energy. The maximum values are 0.36859 and 0.28439 cm^2/g at 80 and 356 keV energy. In comparison with the pure CE resin, the gamma radiation shielding capacity of the CE/MCs composite material was improved by up to 303.05% and 114.86% at 80 and 356 keV energy. Meanwhile, the values at 662 keV energy are 0.08153, 0.07634, 0.08161, 0.09059, 0.09412, and 0.08746 cm^2/g at CE/MCs composites with different microcapsule contents. When the effect of density is taken into account, the shielding performance of the CE/MCs composites with small amount of microcapsules is not as good as that of pure resin. However, the shielding performance of CE/MCs with 10.0 wt% microcapsules is still improved by 15.44% compared to pure CE resin. These results prove that the reasonable addition of microcapsule fillers can significantly improve the gamma radiation shielding performance of the composites.

4 | CONCLUSIONS

In this work, we have developed a novel microcapsule and its CE resin-based composites. The microcapsules, prepared by self-assembly method and in-situ precipitation method, consist of EP resin core and PWO shell.

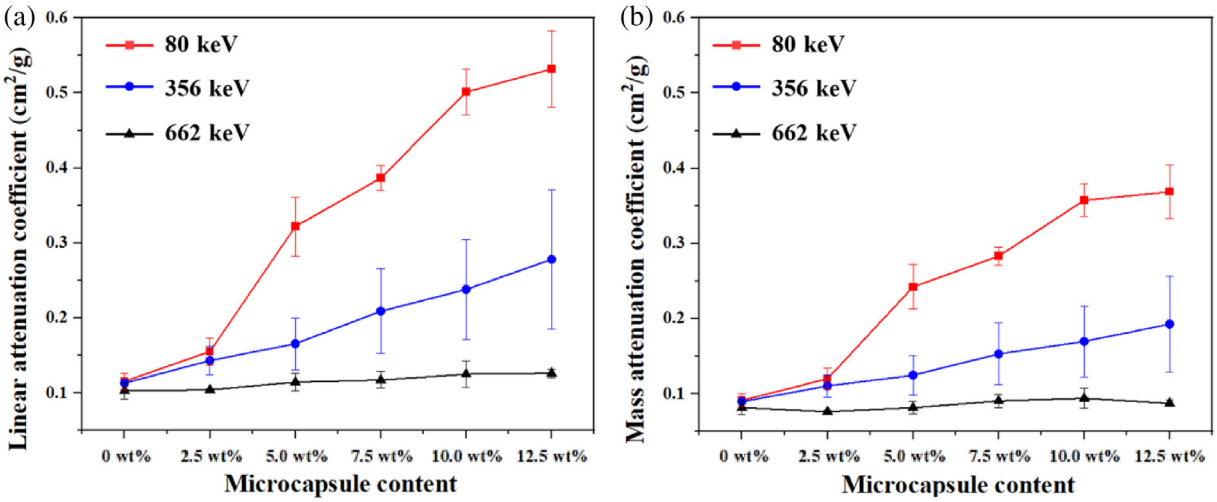

FIGURE 9 (a) Linear attenuation coefficient and (b) mass attenuation coefficient of the CE/MCs composites with different contents of microcapsules for different gamma radiation energies. CE/MCs, cyanate ester resin-based composites containing microcapsules [Color figure can be viewed at wileyonlinelibrary.com]

Meanwhile, the composite material consists of microcapsules, CE resin, and DDS. When microcracks occur in the material, the healing agent EP resin is released from the microcapsules and reacts with the curing agent DDS in the CE resin matrix to repair the microcracks. The PWO shell imparts good thermal stability and encapsulation properties to the microcapsules. In comparison with pure CE resin, the fracture toughness of the CE/MCs composites can increase by 66.5%, and the self-healing efficiency can reach up to 56%, indicating that the microcapsules have good toughening and self-healing abilities. The higher linear and mass attenuation coefficient for the gamma radiation of the CE/MCs composites indicates the good gamma radiation shielding properties of the microcapsules. Therefore, our work provides a new microcapsule and its resin-based composite material with self-healing ability and gamma radiation shielding ability, where the CE/MCs composite with 7.5 wt% microcapsule has the best self-healing performance, excellent fracture toughness and gamma radiation shielding ability.

AUTHOR CONTRIBUTIONS

Yuehao Rui: Conceptualization (lead); investigation (lead); methodology (lead); writing – original draft (lead). **Feida Chen:** Data curation (lead); formal analysis (lead); validation (lead); writing – review and editing (lead). **Minghao Zhao:** Visualization (lead). **Jing Zhong:** Investigation (supporting); software (lead). **Yong Li:** Resources (lead).

ACKNOWLEDGMENTS

The authors would like to thank Xiaodong Chen and Yifan Yang of Nanjing University of Aeronautics and Astronautics for the help in materials preparation. In addition, this work was supported by Postdoctoral Research Foundation of China (grant no. 2020M671488), the Fundamental Research Funds for the Central Universities (grant no. NS2021036), and Postgraduate Research & Practice Innovation Program of NUAA (grant no. xcxjh20210622).

CONFLICT OF INTEREST

The authors declare no conflict of interest.

DATA AVAILABILITY STATEMENT

The data that support the findings of this study are available on request from the corresponding author. The data are not publicly available due to privacy or ethical restrictions.

ORCID

Feida Chen https://orcid.org/0000-0002-5939-5217
Xiaobin Tang https://orcid.org/0000-0003-3308-0468

REFERENCES

[1] M. Naito, S. Kodaira, R. Ogawara, K. Tobita, Y. Someya, T. Kusumoto, H. Kusano, H. Kitamura, M. Koike, Y. Uchihori, *Life Sci. Space Res.* **2020**, *26*, 69.
[2] M. Naito, H. Kitamura, M. Koike, H. Kusano, T. Kusumoto, Y. Uchihori, T. Endo, Y. Hagiwara, N. Kiyono, H. Kodama, *Life Sci. Space Res.* **2021**, *31*, 71.
[3] K. Sairajan, P. Nair, *Compos. Part B. Eng.* **2011**, *42*, 280.
[4] S. M. Li, Y. F. Zhu, Y. Wang, B. R. Wang, Y. D. Huang, T. Yu, *Compos. Commun.* **2021**, *23*.
[5] L. L. Wang, F. H. Zhang, Y. J. Liu, J. S. Leng, *Smart Mater. Struct.* **2019**, *28*, 7.
[6] D. Petry, C. Grunwald, A. Lohberg, A. Brandl, C. Oxynos-Lauschke, T. Andreev, R. van der Ven, U. Schuhmacher, S. Fugger, A. Caon, presented at 9th Eur. Sp. Power. Conf, France, October **2011**.
[7] P. C. Chen, C. W. Bowers, D. A. Content, M. Marzouk, R. C. Romeo, *Opt. Eng.* **2000**, *39*, 2320.
[8] S. L. Xu, S. L. Zou, Y. C. Han, T. Y. Zhang, Y. T. Qu, *IEEE Sensors J.* **2019**, *19*, 6729.
[9] M. Jean-St-Laurent, M. L. Dano, M. J. Potvin, *J. Compos. Mater.* **2017**, *51*, 2023.
[10] J. Ajaja, F. Barthelat, *Compos. Part B. Eng.* **2016**, *90*, 523.
[11] S. Duzellier, P. Gordo, R. Melicio, D. Valerio, M. Millinger, A. Amorim, *Acta Astronaut.* **2022**, *192*, 258.
[12] Y. F. Lu, Q. Shao, H. H. Yue, F. Yang, *IEEE Access.* **2019**, *7*, 93473.
[13] W. Qin, D. Q. Peng, X. H. Wu, J. H. Liao, *Nucl. Instrum. Method B* **2014**, *325*, 115.
[14] F. Garcia, K. Kurvinen, T. Brander, R. Orava, J. Heino, A. Virtanen, H. Kettunen, M. Tenhunen, presented at *IEEE. Nucl. Sci. Symp. Conf. Rec.,* San Diego, CA, February **2007**.
[15] J. G. Huang, P. Li, W. H. Hu, R. K. Du, G. Z. Zhao, Z. Wang, *J. Appl. Polym. Sci.* **2020**, *137*, 45.
[16] J. F. Liu, W. F. Fan, G. W. Lu, D. F. Zhou, Z. Wang, J. L. Yan, *Polymers* **2019**, *11*, 5.
[17] A. Inamdar, J. Cherukattu, A. Anand, B. Kandasubramanian, *Ind. Eng. Chem. Res.* **2018**, *57*, 4479.
[18] X. D. Sun, M. F. Zeng, C. Y. Lu, F. Y. Yan, C. Z. Qi, *Polym. Plast. Technol.* **2010**, *49*, 772.
[19] Y. Feng, Z. P. Fang, A. J. Gu, *Polym. Adv. Technol.* **2004**, *15*, 628.
[20] L. Chen, D. X. Ren, S. J. Chen, H. Pan, M. Z. Xu, X. B. Liu, *Express Polym Lett* **2019**, *13*, 456.
[21] D. X. Zhuo, A. J. Gu, G. Z. Liang, J. T. Hu, L. Yuan, L. F. Ji, *Polym. Int.* **2011**, *60*, 1277.
[22] S. Chen, L. Yuan, Z. H. Wang, A. J. Gu, G. Z. Liang, *Compos. Part B. Eng.* **2019**, *177*, 107438.
[23] S. Myhre, J. Labor, *J. Aircr.* **1981**, *18*, 546.
[24] M. Kessler, N. R. Sottos, S. R. White, *Compos. Part A. Appl. Sci.* **2003**, *34*, 743.
[25] D. G. Bekas, K. Tsirka, D. Baltzis, A. S. Paipetis, *Compos. Part B. Eng.* **2016**, *87*, 92.
[26] S. R. White, N. R. Sottos, P. H. Geubelle, J. S. Moore, M. R. Kessler, S. Sriram, E. N. Brown, S. Viswanathan, *Nature* **2001**, *409*, 794.
[27] L. Yuan, S. Huang, A. J. Gu, G. Z. Liang, F. Chen, Y. Hu, S. Nutt, *Compos. Sci. Technol.* **2013**, *87*, 111.
[28] J. W. Gu, X. T. Yang, C. M. Li, K. C. Kou, *Ind. Eng. Chem. Res.* **2016**, *55*, 10941.

[29] N. J. AbuAlRoos, N. A. B. Amin, R. Zainon, *Radiat. Phys. Chem.* **2019**, *165*, 108439.
[30] L. Lou, Z. Jiang, Q. Zhang, D. Liu, Y. Zhou, K. Zhang, R. He, J. Fan, H. Yan, W. Yang, *Int. J. Energy Res.* **2019**, *43*, 8398.
[31] M. Goyal, S. N. Agarwal, N. Bhatnagar, *J. Appl. Polym. Sci.* **2022**, *139*, e52816.
[32] W. Li, T. B. Tang, *Prog. Cryst. Growth. Ch.* **2000**, *40*, 177.

How to cite this article: Y. Rui, F. Chen, M. Zhao, J. Zhong, Y. Li, X. Tang, *J. Appl. Polym. Sci.* **2022**, e53260. https://doi.org/10.1002/app.53260